

# Implementation of CNOT and Toffoli gates with higher-dimensional spaces

Wen-Qiang Liu<sup>1,2</sup>, Hai-Rui Wei<sup>1,\*</sup>, Leong-Chuan Kwek<sup>3,4,5</sup>

**1** School of Mathematics and Physics, University of Science and Technology Beijing, Beijing 100083, China

**2** Center for Quantum Technology Research and Key Laboratory of Advanced Optoelectronic Quantum Architecture and Measurements (MOE), School of Physics, Beijing Institute of Technology, Beijing 100081, China

**3** Centre for Quantum Technologies, National University of Singapore, Singapore 117543, Singapore

**4** MajuLab, CNRS-UNS-NUS-NTU International Joint Research Unit, Singapore UMI 3654, Singapore

**5** National Institute of Education and Institute of Advanced Studies, Nanyang Technological University, Singapore 637616, Singapore

\* hrwei@ustb.edu.cn

July 20, 2021

## Abstract

Minimizing the number of necessary two-qubit gates is an important task in quantum information processing. By introducing non-computational quantum states in auxiliary spaces, we construct effective circuits for the controlled-NOT (CNOT) gate and the  $n$ -control-qubit Toffoli gate with  $(2n - 1)$  qubit-qudit gates and  $(2n - 2)$  single-qudit gates. We propose the polarization CNOT and Toffoli gates based on the designed quantum circuits in linear optics by operating on the spatial-mode degree of freedom of photons. Our optical schemes can be achieved with a higher success probability and no extra auxiliary photons are needed.

## Contents

<b>1</b>	<b>Introduction</b>	<b>2</b>
<b>2</b>	<b>Construction of CNOT and Toffoli gates with higher-dimensional spaces</b>	<b>3</b>
2.1	Synthesis of a CNOT gate using qutrits	3
2.2	Construction of Toffoli gates with higher-dimensional spaces	4
2.2.1	Synthesis of a three-qubit Toffoli gate using qutrits	4
2.2.2	Synthesis of $n$ -control-qubit Toffoli gate using qudits	5
<b>3</b>	<b>Implementation of CNOT and Toffoli gates with linear optics</b>	<b>5</b>
3.1	Implementation of a P-SWAP gate with linear optics	5
3.2	Implementation of a CNOT gate with linear optics	9
3.3	Implementation of a Toffoli gate with linear optics	11

<b>4 Discussion and Conclusion</b>	<b>14</b>
<b>References</b>	<b>16</b>

---

## 1 Introduction

Multi-qubit quantum gates have complex structures and play an important role in quantum computing [1], quantum algorithms [2–5], cryptography [6], etc. [7]. The most popular paradigm for implementing a quantum gate is the quantum circuit model [1, 8]. Quantum circuits can be realized by sequences of two-qubit gates and single-qubit gates in principle [1]. The cost (also called complexity) of the quantum circuits usually is measured by the number of the two-qubit entangled gates involved in the quantum circuit, because they introduce more imperfections and more demands than the single-qubit gates. However, when the cost of a quantum circuit is high, it is difficult to perform the experiments because of the low computing fidelity and limited coherence time. Moreover, the cost of a universal quantum circuit increases exponentially with the accumulation of the number of qubits. The theoretical lower bound for simulating an  $n$ -qubit universal quantum circuit is  $(4^n - 3n - 1)/4$  controlled-NOT (CNOT) gates in qubit system [9]. Hence, it is crucial to find an effective method for building a universal quantum circuit in the simplest possible way.

Several matrix decomposition techniques have been introduced to optimize a large-scale quantum circuit [10–16]. Two-qubit universal quantum circuits have also been constructed with the lowest cost (resources) in qubit systems [9, 17–19]. However, there is still a gap between the current best result [13] and the theoretical lower bound [9] for a multi-qubit universal quantum circuit. Fortunately, Ralph *et al.* [20] found that the quantum circuit may be optimized further by using higher-dimensional Hilbert spaces, and this proposal was later experimentally demonstrated in optical [21] and superconducting systems [22]. Following this, Liu *et al.* [23, 24] reduced the cost of the  $n$ -qubit universal circuit to  $(5/16) \times 4^n - (5/4) \times 2^n + 2n$  CNOT gates when  $n$  was even and  $(5/16) \times 4^n - 2^n + 2(n - 1)$  CNOTs when  $n$  was odd. Liu *et al.* simplified a Fredkin gate from eight CNOTs to five CNOTs [25] or three qubit-qudit gates [26]. In addition, higher-dimensional quantum systems have also been studied [27, 28] and applied in quantum computing [29–32], quantum communication [33–40], and quantum metrology [41].

The Toffoli (controlled-NOT-NOT) gate, a three-qubit conditional operation, is one of the most popular universal multi-qubit quantum gates [42]. It is also an essential component in complex quantum algorithms [2–5], quantum error correction [43, 44], and quantum fault tolerance [45, 46]. In 1995, Barenco *et al.* [1] proposed a concrete construction of a three-qubit Toffoli gate with five two-qubit entangled gates. When two-qubit gates are restricted to CNOT gates, the optimal cost of a Toffoli gate increases to six [47]. In 2013, Yu *et al.* [48, 49] confirmed that the minimum resource for simulating a three-qubit Toffoli gate is five two-qubit gates. In 2020, Kiktenko *et al.* [50] constructed a generalized  $m$ -qubit Toffoli gate with  $(2m - 3)$  CNOTs based on qudits. Independent of the standard decomposition-based approach, Toffoli gates have been implemented experimentally in superconducting circuits [22, 44], linear optics [21, 29, 51–53], trapped ions [54], atoms [55, 56], and quantum dots [57].

Ralph *et al.* [20, 21] first proposed an interesting scheme for synthesizing a Toffoli gate using three qubit-qudit CNOT gates and two single-qutrit  $X_A$  gates. The main idea of the works in Refs. [20, 21] was to extend temporarily the higher-dimensional subspaces on one of the controlled qubit carriers and then perform corresponding logical operations. Using the same method as Refs. [20, 21], in this paper, we propose an alternative scheme to implement the CNOT and Toffoli gates based on the partial-swap (P-SWAP) gates by using higher-dimensional spaces. Specifically,  $(2n - 1)$  qubit-qudit and  $(2n - 2)$  single-qudit gates are required to implement an  $n$ -control-qubit Toffoli gate. In addition, using the spatial-mode degree of freedom (DOF) of the single-photon, we design a feasible optical architecture for implementing CNOT and Toffoli gates with linear optics. Our proposals have several other advantages: (i) Our optical implementation of the CNOT gate does not require an extra entangled photon pair or a single-photon, and the success probability of the gate is enhanced. (ii) Linear optical Toffoli gates can be constructed with a higher success probability than other existing optical schemes [20, 21, 58]. (iii) Our schemes are simple and feasible with the current technology.

## 2 Construction of CNOT and Toffoli gates with higher-dimensional spaces

### 2.1 Synthesis of a CNOT gate using qutrits

A CNOT gate with two P-SWAP gates using qutrits is shown in Fig. 1. The gate qubits are encoded on two computational states,  $|0\rangle$  and  $|1\rangle$ . The single-qutrit  $X_A$  gate provides a three-dimensional subspace on the control qubit. In the following, we describe the construction process of our protocol in detail.

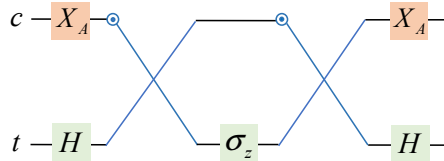


Figure 1: Synthesis of a CNOT gate. The single-qutrit  $X_A$  gate implements the transformation  $|1\rangle \leftrightarrow |2\rangle$ . The controlled node  $\odot$  is turned on for the input  $|0\rangle$  or  $|1\rangle$ . That is, a swap operation is applied to  $c$  and  $t$ , if and only if, the control qubit  $c$  is in the state  $|0\rangle$  or  $|1\rangle$ .  $H$  is a single-qubit Hardmard gate to achieve operations  $|0\rangle \leftrightarrow \frac{1}{\sqrt{2}}(|0\rangle + |1\rangle)$  and  $|1\rangle \leftrightarrow \frac{1}{\sqrt{2}}(|0\rangle - |1\rangle)$ .  $\sigma_z$  completes  $\sigma_z|0\rangle = |0\rangle$  and  $\sigma_z|1\rangle = -|1\rangle$ .

Suppose that the state of the system is initially

$$|\phi_0\rangle = \alpha_1|0_c\rangle|0_t\rangle + \alpha_2|0_c\rangle|1_t\rangle + \alpha_3|1_c\rangle|0_t\rangle + \alpha_4|1_c\rangle|1_t\rangle. \quad (1)$$

where  $\alpha_i$  ( $i = 1, 2, 3, 4$ ) are complex coefficients that satisfy the normalization condition  $\sum_{i=1}^4 |\alpha_i|^2 = 1$ . Subscripts  $c$  and  $t$  denote the control and target qubits, respectively.

First, qubit  $c$  undergoes a single-qutrit gate  $X_A$ , which introduces an ancillary state  $|2\rangle$  on  $c$  and completes the transformations  $|1_c\rangle \xleftrightarrow{X_A} |2_c\rangle$  and  $|0_c\rangle \xleftrightarrow{X_A} |0_c\rangle$ . After the  $X_A$  gate

and a Hadamard ( $H$ ) gate are applied to  $c$  and  $t$ , the initial state  $|\phi_0\rangle$  is changed to

$$|\phi_1\rangle = \frac{1}{\sqrt{2}} [\alpha_1|0_c\rangle(|0_t\rangle + |1_t\rangle) + \alpha_2|0_c\rangle(|0_t\rangle - |1_t\rangle) + \alpha_3|2_c\rangle(|0_t\rangle + |1_t\rangle) + \alpha_4|2_c\rangle(|0_t\rangle - |1_t\rangle)]. \quad (2)$$

Second, a P-SWAP gate is applied to  $c$  and  $t$ , and it transforms  $|\phi_1\rangle$  into

$$|\phi_2\rangle = \frac{1}{\sqrt{2}} [\alpha_1(|0_c\rangle + |1_c\rangle)|0_t\rangle + \alpha_2(|0_c\rangle - |1_c\rangle)|0_t\rangle + \alpha_3|2_c\rangle(|0_t\rangle + |1_t\rangle) + \alpha_4|2_c\rangle(|0_t\rangle - |1_t\rangle)]. \quad (3)$$

Here, the P-SWAP gate performs a swap operation only between two computational states  $|0\rangle$  and  $|1\rangle$ , that is,

$$\begin{aligned} |00\rangle &\xrightarrow{\text{P-SWAP}} |00\rangle, & |01\rangle &\xrightarrow{\text{P-SWAP}} |10\rangle, \\ |10\rangle &\xrightarrow{\text{P-SWAP}} |01\rangle, & |11\rangle &\xrightarrow{\text{P-SWAP}} |11\rangle, \\ |20\rangle &\xrightarrow{\text{P-SWAP}} |20\rangle, & |21\rangle &\xrightarrow{\text{P-SWAP}} |21\rangle. \end{aligned} \quad (4)$$

Third, a  $\sigma_z$  operation acts on  $t$  to change  $|\phi_2\rangle$  to

$$|\phi_3\rangle = \frac{1}{\sqrt{2}} [\alpha_1(|0_c\rangle + |1_c\rangle)|0_t\rangle + \alpha_2(|0_c\rangle - |1_c\rangle)|0_t\rangle + \alpha_3|2_c\rangle(|0_t\rangle - |1_t\rangle) + \alpha_4|2_c\rangle(|0_t\rangle + |1_t\rangle)]. \quad (5)$$

Finally, after the P-SWAP gate, the  $X_A$  gate and  $H$  operation are applied to  $c$  and  $t$  again,  $|\phi_3\rangle$  is changed to

$$|\phi_4\rangle = \alpha_1|0_c\rangle|0_t\rangle + \alpha_2|0_c\rangle|1_t\rangle + \alpha_3|1_c\rangle|1_t\rangle + \alpha_4|1_c\rangle|0_t\rangle. \quad (6)$$

Note that Eq. (6) is a CNOT gate, and such a construction can be achieved in linear optics with a high success probability and without additional photons (see Sec. 3).

## 2.2 Construction of Toffoli gates with higher-dimensional spaces

### 2.2.1 Synthesis of a three-qubit Toffoli gate using qutrits

Based on the designed CNOT and P-SWAP gates, the process for implementing a three-qubit Toffoli gate with four-dimensional space is presented in Fig. 2.

Considering an arbitrary normalization three-qubit initial state

$$|\psi_0\rangle = \alpha_1|0_{c_1}\rangle|0_{c_2}\rangle|0_t\rangle + \alpha_2|0_{c_1}\rangle|0_{c_2}\rangle|1_t\rangle + \alpha_3|0_{c_1}\rangle|1_{c_2}\rangle|0_t\rangle + \alpha_4|0_{c_1}\rangle|1_{c_2}\rangle|1_t\rangle + \alpha_5|1_{c_1}\rangle|0_{c_2}\rangle|0_t\rangle + \alpha_6|1_{c_1}\rangle|0_{c_2}\rangle|1_t\rangle + \alpha_7|1_{c_1}\rangle|1_{c_2}\rangle|0_t\rangle + \alpha_8|1_{c_1}\rangle|1_{c_2}\rangle|1_t\rangle. \quad (7)$$

First, the  $X_A$  gate acts on  $c_2$  to achieve  $|1_{c_2}\rangle \xleftrightarrow{X_A} |2_{c_2}\rangle$  and  $|0_{c_2}\rangle \xleftrightarrow{X_A} |0_{c_2}\rangle$ . After the first P-SWAP gate is executed on  $c_1$  and  $c_2$ ,  $|\psi_0\rangle$  becomes

$$|\psi_1\rangle = \alpha_1|0_{c_1}\rangle|0_{c_2}\rangle|0_t\rangle + \alpha_2|0_{c_1}\rangle|0_{c_2}\rangle|1_t\rangle + \alpha_3|0_{c_1}\rangle|2_{c_2}\rangle|0_t\rangle + \alpha_4|0_{c_1}\rangle|2_{c_2}\rangle|1_t\rangle + \alpha_5|0_{c_1}\rangle|1_{c_2}\rangle|0_t\rangle + \alpha_6|0_{c_1}\rangle|1_{c_2}\rangle|1_t\rangle + \alpha_7|1_{c_1}\rangle|2_{c_2}\rangle|0_t\rangle + \alpha_8|1_{c_1}\rangle|2_{c_2}\rangle|1_t\rangle. \quad (8)$$

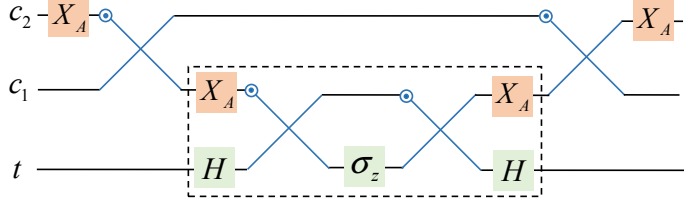


Figure 2: Simplified synthesis of a three-qubit Toffoli gate with two P-SWAP and one CNOT gates. As shown in Fig. 1, the operations in the dotted rectangle are a CNOT gate.

Second, a CNOT gate is applied to  $c_1$  and  $t$  (which can be achieved by the circuit in the dotted rectangle), resulting in

$$|\psi_2\rangle = \alpha_1|0_{c_1}\rangle|0_{c_2}\rangle|0_t\rangle + \alpha_2|0_{c_1}\rangle|0_{c_2}\rangle|1_t\rangle + \alpha_3|0_{c_1}\rangle|2_{c_2}\rangle|0_t\rangle + \alpha_4|0_{c_1}\rangle|2_{c_2}\rangle|1_t\rangle + \alpha_5|0_{c_1}\rangle|1_{c_2}\rangle|0_t\rangle + \alpha_6|0_{c_1}\rangle|1_{c_2}\rangle|1_t\rangle + \alpha_7|1_{c_1}\rangle|2_{c_2}\rangle|1_t\rangle + \alpha_8|1_{c_1}\rangle|2_{c_2}\rangle|0_t\rangle. \quad (9)$$

Finally, the P-SWAP and  $X_A$  gates are applied again. The two operations induce  $|\psi_2\rangle$  as the final state

$$|\psi_3\rangle = \alpha_1|0_{c_1}\rangle|0_{c_2}\rangle|0_t\rangle + \alpha_2|0_{c_1}\rangle|0_{c_2}\rangle|1_t\rangle + \alpha_3|0_{c_1}\rangle|1_{c_2}\rangle|0_t\rangle + \alpha_4|0_{c_1}\rangle|1_{c_2}\rangle|1_t\rangle + \alpha_5|1_{c_1}\rangle|0_{c_2}\rangle|0_t\rangle + \alpha_6|1_{c_1}\rangle|0_{c_2}\rangle|1_t\rangle + \alpha_7|1_{c_1}\rangle|1_{c_2}\rangle|1_t\rangle + \alpha_8|1_{c_1}\rangle|1_{c_2}\rangle|0_t\rangle. \quad (10)$$

From Eqs. (7-10), one can see that a three-qubit Toffoli gate can be simulated using three nearest-neighbor qubit-qudit gates and two single-qutrit gates.

### 2.2.2 Synthesis of $n$ -control-qubit Toffoli gate using qudits

Using a higher-dimensional space, the method can be applied to any multi-qubit Toffoli gate. As shown in Fig. 3, an  $n$ -control-qubit Toffoli gate is constructed with  $(2n-1)$  qubit-qudit and  $(2n-2)$  single-qudit gates, which flips the target qubit states  $|0\rangle$  and  $|1\rangle$  if and only if the  $n$  control-qubits are all  $|1\rangle$ . Here, single-qudit gates  $X_a, X_b, \dots, X_n$  create multi-level qudits on  $c_n$  and complete transformations  $|0_{c_n}\rangle \leftrightarrow |2_{c_n}\rangle, |1_{c_n}\rangle \leftrightarrow |3_{c_n}\rangle, |0_{c_n}\rangle \leftrightarrow |4_{c_n}\rangle, \dots, |0_{c_n}\rangle \leftrightarrow |n_{c_n}\rangle$  when  $n$  is even or  $|0_{c_n}\rangle \leftrightarrow |2_{c_n}\rangle, |1_{c_n}\rangle \leftrightarrow |3_{c_n}\rangle, |0_{c_n}\rangle \leftrightarrow |4_{c_n}\rangle, \dots, |1_{c_n}\rangle \leftrightarrow |n_{c_n}\rangle$  when  $n$  is odd. These single-qudit gates can temporarily expand the two-dimensional space of  $c_n$  to an  $(n+1)$ -dimensional subspace. All CNOT and P-SWAP gates act on computational states  $|0\rangle$  and  $|1\rangle$ . The synthesis requires only  $O(n)$  qubit-qudit gates and the low-cost advantage is more evident in our scheme as the number of qubits increases.

## 3 Implementation of CNOT and Toffoli gates with linear optics

### 3.1 Implementation of a P-SWAP gate with linear optics

In the previous section, we proposed the simulation of CNOT and Toffoli gates based on P-SWAP gates and auxiliary higher-dimensional spaces. In an optical system, two computational states can be encoded on the polarization DOF of a single photon in the spatial-mode  $i$ , that is,  $|0\rangle \equiv |H\rangle_i$  and  $|1\rangle \equiv |V\rangle_i$ . Here,  $H$  and  $V$  represent the horizontal and vertical polarized

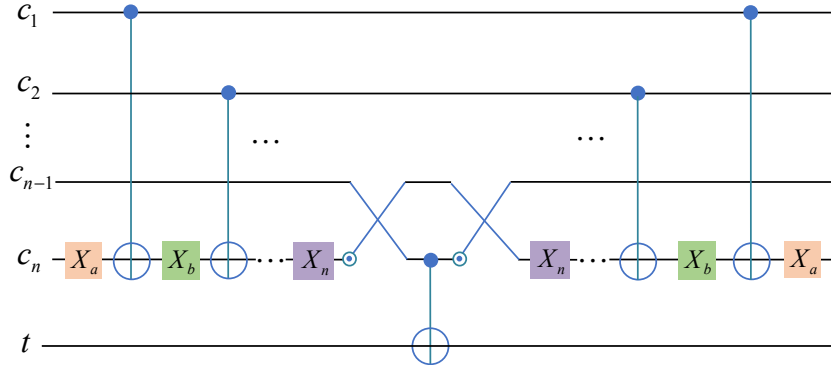


Figure 3: Synthesis of an  $n$ -control-qubit Toffoli gate in a higher-dimensional space. Single-qudit gates  $X_a, X_b, \dots, X_n$  complete operations  $|0_{c_n}\rangle \leftrightarrow |2_{c_n}\rangle, |1_{c_n}\rangle \leftrightarrow |3_{c_n}\rangle, \dots, |0_{c_n}\rangle \leftrightarrow |n_{c_n}\rangle$  when  $n$  is even or  $|0_{c_n}\rangle \leftrightarrow |2_{c_n}\rangle, |1_{c_n}\rangle \leftrightarrow |3_{c_n}\rangle, \dots, |1_{c_n}\rangle \leftrightarrow |n_{c_n}\rangle$  when  $n$  is odd, respectively.

components, respectively. The higher-dimensional state can be encoded on the  $V$ -polarized component in a new spatial-mode  $i'$ , that is,  $|2\rangle \equiv |V\rangle_{i'}$ . The qutrit operation  $X_A$  can be achieved by employing a polarizing beam splitter (PBS), which reflects the  $V$ -polarized component and transmits the  $H$ -polarized component, respectively. Before describing the implementation of the CNOT gate, we first detail the step-by-step construction of the P-SWAP gate with linear optical elements.

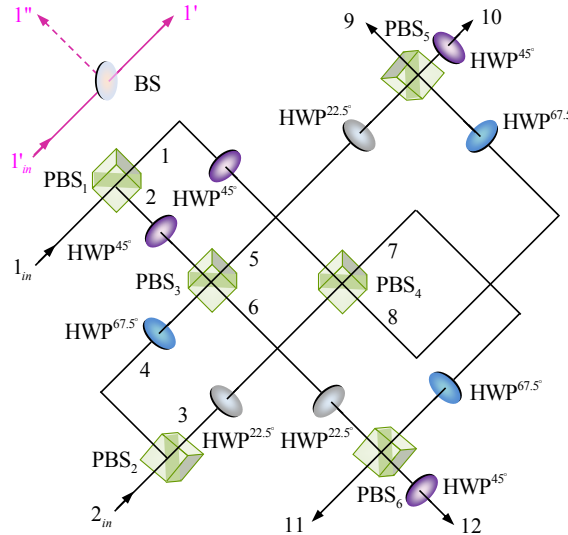


Figure 4: Implementation of a linear optical P-SWAP gate. The half-wave plate  $\text{HWP}^{45^\circ}$  realizes the qubit-flip  $\hat{a}_H^\dagger \leftrightarrow \hat{a}_V^\dagger$ .  $\text{HWP}^{22.5^\circ}$  completes the operations  $\hat{a}_H^\dagger \leftrightarrow \frac{1}{\sqrt{2}}(\hat{a}_H^\dagger + \hat{a}_V^\dagger)$  and  $\hat{a}_V^\dagger \leftrightarrow \frac{1}{\sqrt{2}}(\hat{a}_H^\dagger - \hat{a}_V^\dagger)$ , and  $\text{HWP}^{67.5^\circ}$  completes  $\hat{a}_H^\dagger \leftrightarrow \frac{1}{\sqrt{2}}(-\hat{a}_H^\dagger + \hat{a}_V^\dagger)$  and  $\hat{a}_V^\dagger \leftrightarrow \frac{1}{\sqrt{2}}(\hat{a}_H^\dagger + \hat{a}_V^\dagger)$ . BS is a balanced beam splitter to realize  $\hat{a}_{V_{1'} in}^\dagger \leftrightarrow \frac{1}{\sqrt{2}}(\hat{a}_{V_1'}^\dagger + \hat{a}_{V_1''}^\dagger)$ .

As shown in Fig. 4, the injected photon 1 is divided into  $H$ -polarized component and

*V*-polarized component by a PBS. The *H*-polarized component passes into the spatial-mode  $1_{in}$ , which is encoded on  $|H\rangle_{1_{in}} \equiv |0\rangle$  (and *V*-polarized component in the spatial-mode  $1_{in}$  is encoded on  $|V\rangle_{1_{in}} \equiv |1\rangle$ ), while the *V*-polarized component is reflected into another spatial-mode  $1'_{in}$ , which is encoded on  $|V\rangle_{1'_{in}} \equiv |2\rangle$ . The photon 2 from the spatial-mode  $2_{in}$  is encoded on  $|H\rangle_{2_{in}} \equiv |0\rangle$  and  $|V\rangle_{2_{in}} \equiv |1\rangle$ . A general injected photon state can be considered as

$$|\varphi_0\rangle = (\alpha_1 \hat{a}_{H_{1_{in}}}^\dagger \hat{a}_{H_{2_{in}}}^\dagger + \alpha_2 \hat{a}_{H_{1_{in}}}^\dagger \hat{a}_{V_{2_{in}}}^\dagger + \alpha_3 \hat{a}_{V_{1_{in}}}^\dagger \hat{a}_{H_{2_{in}}}^\dagger + \alpha_4 \hat{a}_{V_{1_{in}}}^\dagger \hat{a}_{V_{2_{in}}}^\dagger + \alpha_5 \hat{a}_{V_{1'_{in}}}^\dagger \hat{a}_{H_{2_{in}}}^\dagger + \alpha_6 \hat{a}_{V_{1'_{in}}}^\dagger \hat{a}_{V_{2_{in}}}^\dagger) |\text{vac.}\rangle. \quad (11)$$

Here  $|\text{vac.}\rangle$  is the state vector of vacuum.

First, PBS<sub>1</sub> and PBS<sub>2</sub> transmit the *H*-photons into modes 1 and 3 to interact with half-wave plates HWP<sup>45°</sup> and HWP<sup>22.5°</sup> and reflect the *V*-photons into modes 2 and 4 to interact with HWP<sup>45°</sup> and HWP<sup>67.5°</sup>. Here, HWP<sup>45°</sup> is a half-wave plate set to 45 degrees and achieves the qubit-flip operation  $\hat{a}_H^\dagger \leftrightarrow \hat{a}_V^\dagger$ . HWP<sup>22.5°</sup> completes the transformations

$$\hat{a}_H^\dagger \xrightarrow{\text{HWP}^{22.5^\circ}} \frac{1}{\sqrt{2}}(\hat{a}_H^\dagger + \hat{a}_V^\dagger), \quad \hat{a}_V^\dagger \xrightarrow{\text{HWP}^{22.5^\circ}} \frac{1}{\sqrt{2}}(\hat{a}_H^\dagger - \hat{a}_V^\dagger). \quad (12)$$

HWP<sup>67.5°</sup> results in

$$\hat{a}_H^\dagger \xrightarrow{\text{HWP}^{67.5^\circ}} \frac{1}{\sqrt{2}}(-\hat{a}_H^\dagger + \hat{a}_V^\dagger), \quad \hat{a}_V^\dagger \xrightarrow{\text{HWP}^{67.5^\circ}} \frac{1}{\sqrt{2}}(\hat{a}_H^\dagger + \hat{a}_V^\dagger). \quad (13)$$

The above operations, PBS<sub>1</sub> → HWP<sup>45°</sup> (HWP<sup>45°</sup>) and PBS<sub>2</sub> → HWP<sup>22.5°</sup> (HWP<sup>67.5°</sup>) cause  $|\varphi_0\rangle$  to become

$$|\varphi_1\rangle = \frac{1}{\sqrt{2}} [\alpha_1 \hat{a}_{V_1}^\dagger (\hat{a}_{H_3}^\dagger + \hat{a}_{V_3}^\dagger) + \alpha_2 \hat{a}_{V_1}^\dagger (\hat{a}_{H_4}^\dagger + \hat{a}_{V_4}^\dagger) + \alpha_3 \hat{a}_{H_2}^\dagger (\hat{a}_{H_3}^\dagger + \hat{a}_{V_3}^\dagger) + \alpha_4 \hat{a}_{H_2}^\dagger (\hat{a}_{H_4}^\dagger + \hat{a}_{V_4}^\dagger) + \alpha_5 \hat{a}_{V_{1'_{in}}}^\dagger (\hat{a}_{H_3}^\dagger + \hat{a}_{V_3}^\dagger) + \alpha_6 \hat{a}_{V_{1'_{in}}}^\dagger (\hat{a}_{H_4}^\dagger + \hat{a}_{V_4}^\dagger)] |\text{vac.}\rangle. \quad (14)$$

Second, photons in mode  $1'_{in}$  are then split into modes  $1'$  and  $1''$  by a balanced polarization beam splitter (BS), i.e.,  $\hat{a}_{V_{1'_{in}}}^\dagger \xrightarrow{\text{BS}} (\hat{a}_{V_{1'}}^\dagger + \hat{a}_{V_{1''}}^\dagger)/\sqrt{2}$ . Photons emitted from modes 2 and 4 (1 and 3) are split into modes 5 and 6 (7 and 8) by PBS<sub>3</sub> (PBS<sub>4</sub>) and followed by HWP<sup>22.5°</sup> (HWP<sup>67.5°</sup>). These elements change  $|\varphi_1\rangle$  as

$$|\varphi_2\rangle = \frac{1}{2\sqrt{2}} [\alpha_1 (\hat{a}_{H_7}^\dagger + \hat{a}_{V_7}^\dagger)(-\hat{a}_{H_7}^\dagger + \hat{a}_{V_7}^\dagger + \hat{a}_{H_8}^\dagger + \hat{a}_{V_8}^\dagger) + \alpha_2 (\hat{a}_{H_7}^\dagger + \hat{a}_{V_7}^\dagger)(\hat{a}_{H_5}^\dagger + \hat{a}_{V_5}^\dagger + \hat{a}_{H_6}^\dagger - \hat{a}_{V_6}^\dagger) + \alpha_3 (\hat{a}_{H_6}^\dagger + \hat{a}_{V_6}^\dagger)(-\hat{a}_{H_7}^\dagger + \hat{a}_{V_7}^\dagger + \hat{a}_{H_8}^\dagger + \hat{a}_{V_8}^\dagger) + \alpha_4 (\hat{a}_{H_6}^\dagger + \hat{a}_{V_6}^\dagger)(\hat{a}_{H_5}^\dagger + \hat{a}_{V_5}^\dagger + \hat{a}_{H_6}^\dagger - \hat{a}_{V_6}^\dagger) + \alpha_5 (\hat{a}_{V_{1'}}^\dagger + \hat{a}_{V_{1''}}^\dagger)(-\hat{a}_{H_7}^\dagger + \hat{a}_{V_7}^\dagger + \hat{a}_{H_8}^\dagger + \hat{a}_{V_8}^\dagger) + \alpha_6 (\hat{a}_{V_{1'}}^\dagger + \hat{a}_{V_{1''}}^\dagger)(\hat{a}_{H_5}^\dagger + \hat{a}_{V_5}^\dagger + \hat{a}_{H_6}^\dagger - \hat{a}_{V_6}^\dagger)] |\text{vac.}\rangle. \quad (15)$$

Third, PBS<sub>5</sub> (PBS<sub>6</sub>) induces photons into modes 9 and 10 (11 and 12). Photons in modes 10 and 12 will undergo HWP<sup>45°</sup>. Thus, the state of the system evolves as

$$\begin{aligned} |\varphi_3\rangle = & \frac{1}{2\sqrt{2}} [\alpha_1(\hat{a}_{H_{11}}^\dagger + \hat{a}_{H_{12}}^\dagger)(-\hat{a}_{H_{11}}^\dagger + \hat{a}_{H_{12}}^\dagger + \hat{a}_{H_9}^\dagger + \hat{a}_{H_{10}}^\dagger) \\ & + \alpha_2(\hat{a}_{H_{11}}^\dagger + \hat{a}_{H_{12}}^\dagger)(\hat{a}_{V_{10}}^\dagger + \hat{a}_{V_9}^\dagger + \hat{a}_{V_{12}}^\dagger - \hat{a}_{V_{11}}^\dagger) \\ & + \alpha_3(\hat{a}_{V_{12}}^\dagger + \hat{a}_{V_{11}}^\dagger)(-\hat{a}_{H_{11}}^\dagger + \hat{a}_{H_{12}}^\dagger + \hat{a}_{H_9}^\dagger + \hat{a}_{H_{10}}^\dagger) \\ & + \alpha_4(\hat{a}_{V_{12}}^\dagger + \hat{a}_{V_{11}}^\dagger)(\hat{a}_{V_{10}}^\dagger + \hat{a}_{V_9}^\dagger + \hat{a}_{V_{12}}^\dagger - \hat{a}_{V_{11}}^\dagger) \\ & + \alpha_5(\hat{a}_{V_{1'}}^\dagger + \hat{a}_{V_{1''}}^\dagger)(-\hat{a}_{H_{11}}^\dagger + \hat{a}_{H_{12}}^\dagger + \hat{a}_{H_9}^\dagger + \hat{a}_{H_{10}}^\dagger) \\ & + \alpha_6(\hat{a}_{V_{1'}}^\dagger + \hat{a}_{V_{1''}}^\dagger)(\hat{a}_{V_{10}}^\dagger + \hat{a}_{V_9}^\dagger + \hat{a}_{V_{12}}^\dagger - \hat{a}_{V_{11}}^\dagger)] |vac.\rangle. \end{aligned} \quad (16)$$

The state  $|\varphi_3\rangle$  also has the form

$$\begin{aligned} |\varphi_3\rangle = & |\varphi_4^1\rangle + |\varphi_4^2\rangle + |\varphi_4^3\rangle + |\varphi_4^4\rangle \\ & + \frac{1}{2\sqrt{2}} [\alpha_1(\hat{a}_{H_{11}}^\dagger + \hat{a}_{H_{12}}^\dagger)(-\hat{a}_{H_{11}}^\dagger + \hat{a}_{H_{12}}^\dagger) \\ & + \alpha_2(-\hat{a}_{H_{11}}^\dagger \hat{a}_{V_{11}}^\dagger + \hat{a}_{H_{11}}^\dagger \hat{a}_{V_{12}}^\dagger - \hat{a}_{V_{11}}^\dagger \hat{a}_{H_{12}}^\dagger + \hat{a}_{H_{12}}^\dagger \hat{a}_{V_{12}}^\dagger) \\ & + \alpha_3(-\hat{a}_{H_{11}}^\dagger \hat{a}_{V_{11}}^\dagger + \hat{a}_{V_{11}}^\dagger \hat{a}_{H_{12}}^\dagger - \hat{a}_{H_{11}}^\dagger \hat{a}_{V_{12}}^\dagger + \hat{a}_{H_{12}}^\dagger \hat{a}_{V_{11}}^\dagger) \\ & + \alpha_4(\hat{a}_{V_{12}}^\dagger + \hat{a}_{V_{11}}^\dagger)(\hat{a}_{V_{12}}^\dagger - \hat{a}_{V_{11}}^\dagger) \\ & + \alpha_5(\hat{a}_{V_{1'}}^\dagger + \hat{a}_{V_{1''}}^\dagger)(\hat{a}_{H_9}^\dagger + \hat{a}_{H_{10}}^\dagger) \\ & + \alpha_6(\hat{a}_{V_{1'}}^\dagger + \hat{a}_{V_{1''}}^\dagger)(\hat{a}_{V_9}^\dagger + \hat{a}_{V_{10}}^\dagger)] |vac.\rangle. \end{aligned} \quad (17)$$

Here the four orthogonal states  $|\varphi_4^1\rangle$ ,  $|\varphi_4^2\rangle$ ,  $|\varphi_4^3\rangle$ , and  $|\varphi_4^4\rangle$  are given by

$$\begin{aligned} |\varphi_4^1\rangle = & \frac{1}{2\sqrt{2}} (\alpha_1 \hat{a}_{H_9}^\dagger \hat{a}_{H_{12}}^\dagger + \alpha_2 \hat{a}_{V_9}^\dagger \hat{a}_{H_{12}}^\dagger + \alpha_3 \hat{a}_{H_9}^\dagger \hat{a}_{V_{12}}^\dagger + \alpha_4 \hat{a}_{V_9}^\dagger \hat{a}_{V_{12}}^\dagger \\ & + \alpha_5 \hat{a}_{V_{1'}}^\dagger \hat{a}_{H_{12}}^\dagger + \alpha_6 \hat{a}_{V_{1'}}^\dagger \hat{a}_{V_{12}}^\dagger) |vac.\rangle, \end{aligned} \quad (18)$$

$$\begin{aligned} |\varphi_4^2\rangle = & \frac{1}{2\sqrt{2}} (\alpha_1 \hat{a}_{H_{10}}^\dagger \hat{a}_{H_{12}}^\dagger + \alpha_2 \hat{a}_{V_{10}}^\dagger \hat{a}_{H_{12}}^\dagger + \alpha_3 \hat{a}_{H_{10}}^\dagger \hat{a}_{V_{12}}^\dagger + \alpha_4 \hat{a}_{V_{10}}^\dagger \hat{a}_{V_{12}}^\dagger \\ & + \alpha_5 \hat{a}_{V_{1''}}^\dagger \hat{a}_{H_{12}}^\dagger + \alpha_6 \hat{a}_{V_{1''}}^\dagger \hat{a}_{V_{12}}^\dagger) |vac.\rangle, \end{aligned} \quad (19)$$

$$\begin{aligned} |\varphi_4^3\rangle = & \frac{1}{2\sqrt{2}} (\alpha_1 \hat{a}_{H_9}^\dagger \hat{a}_{H_{11}}^\dagger + \alpha_2 \hat{a}_{V_9}^\dagger \hat{a}_{H_{11}}^\dagger + \alpha_3 \hat{a}_{H_9}^\dagger \hat{a}_{V_{11}}^\dagger + \alpha_4 \hat{a}_{V_9}^\dagger \hat{a}_{V_{11}}^\dagger \\ & - \alpha_5 \hat{a}_{V_{1'}}^\dagger \hat{a}_{H_{11}}^\dagger - \alpha_6 \hat{a}_{V_{1'}}^\dagger \hat{a}_{V_{11}}^\dagger) |vac.\rangle, \end{aligned} \quad (20)$$

$$\begin{aligned} |\varphi_4^4\rangle = & \frac{1}{2\sqrt{2}} (\alpha_1 \hat{a}_{H_{10}}^\dagger \hat{a}_{H_{11}}^\dagger + \alpha_2 \hat{a}_{V_{10}}^\dagger \hat{a}_{H_{11}}^\dagger + \alpha_3 \hat{a}_{H_{10}}^\dagger \hat{a}_{V_{11}}^\dagger + \alpha_4 \hat{a}_{V_{10}}^\dagger \hat{a}_{V_{11}}^\dagger \\ & - \alpha_5 \hat{a}_{V_{1''}}^\dagger \hat{a}_{H_{11}}^\dagger - \alpha_6 \hat{a}_{V_{1''}}^\dagger \hat{a}_{V_{11}}^\dagger) |vac.\rangle. \end{aligned} \quad (21)$$

Based on Eqs. (18-21), one can see that there are four desired coincidence outcomes for the construction of the post-selection P-SWAP gate (see Tab. 1).

- (i) When one chooses the event that photons come from output mode pairs (9, 12) and (1', 12), the state  $|\varphi_3\rangle$  will collapse into  $|\varphi_4^1\rangle$ , and the P-SWAP gate is completed.
- (ii) When one chooses the event that photons come from output mode pairs (10, 12) and (1'', 12), the state  $|\varphi_3\rangle$  will collapse into  $|\varphi_4^2\rangle$ , and the P-SWAP gate is completed.
- (iii) When one chooses the event that photons come from output mode pairs (9, 11) and (1', 11), the state  $|\varphi_3\rangle$  will collapse into  $|\varphi_4^3\rangle$ . And then, a phase flip operation,  $\hat{a}_{V_{1'}}^\dagger \xrightarrow{\sigma_z} -\hat{a}_{V_{1'}}^\dagger$ , should be applied to complete the P-SWAP gate. Such feed-forward operation can be achieved by setting an HWP $0^\circ$  in spatial mode 1'. The spatial-based classical feed-forward operations has been experimentally demonstrated recently [59–62].
- (iv) When one chooses the event that photons come from output mode pairs (10, 11) and (1'', 11), the state  $|\varphi_3\rangle$  will collapse into  $|\varphi_4^4\rangle$ . And then, an HWP $0^\circ$  is set in spatial mode 1'' to complete the P-SWAP gate.

Putting all the pieces together one can find that the quantum circuit shown in Fig. 4 completes a linear optical P-SWAP gate in the coincidence basis with a success probability of  $4 \times 1/8 = 1/2$ . The success (or the output modes) of the scheme can be heralded by using the success instances in the post-selection in the applications.

Table 1: Coincident expectation outgoing values for six logic basis inputs.

	$\hat{a}_{H_9}^\dagger \hat{a}_{H_{12}}^\dagger$	$a_{V_9}^\dagger a_{H_{12}}^\dagger$	$a_{H_9}^\dagger a_{V_{12}}^\dagger$	$a_{V_9}^\dagger a_{V_{12}}^\dagger$	$a_{V_{1'}}^\dagger a_{H_{12}}^\dagger$	$a_{V_{1'}}^\dagger a_{V_{12}}^\dagger$
Input	$a_{H_{10}}^\dagger a_{H_{12}}^\dagger$	$a_{V_{10}}^\dagger a_{H_{12}}^\dagger$	$a_{H_{10}}^\dagger a_{V_{12}}^\dagger$	$a_{V_{10}}^\dagger a_{V_{12}}^\dagger$	$a_{V_{1''}}^\dagger a_{H_{12}}^\dagger$	$a_{V_{1''}}^\dagger a_{V_{12}}^\dagger$
	$a_{H_9}^\dagger a_{H_{11}}^\dagger$	$a_{V_9}^\dagger a_{H_{11}}^\dagger$	$a_{H_9}^\dagger a_{V_{11}}^\dagger$	$a_{V_9}^\dagger a_{V_{11}}^\dagger$	$-a_{V_{1'}}^\dagger a_{H_{11}}^\dagger$	$-a_{V_{1'}}^\dagger a_{V_{11}}^\dagger$
	$a_{H_{10}}^\dagger a_{H_{11}}^\dagger$	$a_{V_{10}}^\dagger a_{H_{11}}^\dagger$	$a_{H_{10}}^\dagger a_{V_{11}}^\dagger$	$a_{V_{10}}^\dagger a_{V_{11}}^\dagger$	$-a_{V_{1''}}^\dagger a_{H_{11}}^\dagger$	$-a_{V_{1''}}^\dagger a_{V_{11}}^\dagger$
	$a_{H_{1_{in}}}^\dagger a_{H_{2_{in}}}^\dagger$	1/8	0	0	0	0
	$a_{H_{1_{in}}}^\dagger a_{V_{2_{in}}}^\dagger$	0	1/8	0	0	0
	$a_{V_{1_{in}}}^\dagger a_{H_{2_{in}}}^\dagger$	0	0	1/8	0	0
	$a_{V_{1_{in}}}^\dagger a_{V_{2_{in}}}^\dagger$	0	0	0	1/8	0
	$a_{V_{1'_{in}}}^\dagger a_{H_{2_{in}}}^\dagger$	0	0	0	0	1/8
	$a_{V_{1'_{in}}}^\dagger a_{V_{2_{in}}}^\dagger$	0	0	0	0	1/8

### 3.2 Implementation of a CNOT gate with linear optics

As shown in Fig. 5, a P-SWAP-based CNOT gate can be realized in the coincidence basis with linear optical elements. PBS plays a role in the qutrit  $X_A$  to provide an additional spatial mode. The operation in the black dotted rectangle corresponds to a P-SWAP gate in Fig. 4.

First, after the two photons are injected into modes 1 and 2, the input state of the system is given by

$$|\chi_0\rangle = (\alpha_1 \hat{a}_{H_1}^\dagger \hat{a}_{H_2}^\dagger + \alpha_2 \hat{a}_{H_1}^\dagger \hat{a}_{V_2}^\dagger + \alpha_3 \hat{a}_{V_1}^\dagger \hat{a}_{H_2}^\dagger + \alpha_4 \hat{a}_{V_1}^\dagger \hat{a}_{V_2}^\dagger) |\text{vac.}\rangle. \quad (22)$$

Second, photons 1 and 2 execute a PBS<sub>1</sub> and an HWP $22.5^\circ$ , respectively, to pass through the first P-SWAP gate. After the photons interact with the first P-SWAP gate, the outing

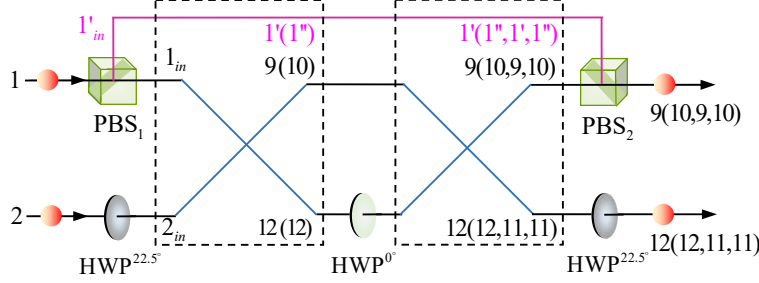


Figure 5: Implementation of a linear optical CNOT gate. The operation in the dotted rectangle is a P-SWAP gate, as shown in Fig. 4. The numbers represent input-output modes and the mode  $i(j)$  of photon 1 corresponds to  $k(n)$  of photon 2 with  $i, j \in \{9, 10\}$  and  $k, n \in \{11, 12\}$ .

photons emitted from spatial mode pairs  $(9, 12)$  and  $(1', 12)$ , or  $(10, 12)$  and  $(1'', 12)$  (as an input) will be led to the next  $HWP^{0^\circ}$  and the rightmost P-SWAP gate.  $PBS_1$ ,  $HWP^{22.5^\circ}$ , and the leftmost P-SWAP gate change  $|\chi_0\rangle$  into  $|\chi_{9,1',12}\rangle$  or  $|\chi_{10,1'',12}\rangle$ . Here,

$$|\chi_{9,1',12}\rangle_1 = \frac{1}{4} [\alpha_1(\hat{a}_{H_9}^\dagger + \hat{a}_{V_9}^\dagger)\hat{a}_{H_{12}}^\dagger + \alpha_2(\hat{a}_{H_9}^\dagger - \hat{a}_{V_9}^\dagger)\hat{a}_{H_{12}}^\dagger + \alpha_3\hat{a}_{V_{1'}}^\dagger(\hat{a}_{H_{12}}^\dagger + \hat{a}_{V_{12}}^\dagger) + \alpha_4\hat{a}_{V_{1''}}^\dagger(\hat{a}_{H_{12}}^\dagger - \hat{a}_{V_{12}}^\dagger)]|vac.\rangle, \quad (23)$$

$$|\chi_{10,1'',12}\rangle_1 = \frac{1}{4} [\alpha_1(\hat{a}_{H_{10}}^\dagger + \hat{a}_{V_{10}}^\dagger)\hat{a}_{H_{12}}^\dagger + \alpha_2(\hat{a}_{H_{10}}^\dagger - \hat{a}_{V_{10}}^\dagger)\hat{a}_{H_{12}}^\dagger + \alpha_3\hat{a}_{V_{1''}}^\dagger(\hat{a}_{H_{12}}^\dagger + \hat{a}_{V_{12}}^\dagger) + \alpha_4\hat{a}_{V_{1'}}^\dagger(\hat{a}_{H_{12}}^\dagger - \hat{a}_{V_{12}}^\dagger)]|vac.\rangle. \quad (24)$$

Third,  $HWP^{0^\circ}$  acts on mode 12 to complete  $\hat{a}_{H_{12}}^\dagger \rightarrow \hat{a}_{H_{12}}^\dagger$  and  $\hat{a}_{V_{12}}^\dagger \rightarrow -\hat{a}_{V_{12}}^\dagger$ . The second P-SWAP gate produces eight desired outcomes of the system, that is, (i) when the outing photons emitted from spatial mode pairs  $(9, 12)$  and  $(1', 12)$ , the state  $|\chi_{9,1',12}\rangle_1$  and  $|\chi_{10,1'',12}\rangle_1$  both become

$$|\chi_{9,1',12}^+\rangle_2 = \frac{1}{8\sqrt{2}} [\alpha_1\hat{a}_{H_9}^\dagger(\hat{a}_{H_{12}}^\dagger + \hat{a}_{V_{12}}^\dagger) + \alpha_2\hat{a}_{H_9}^\dagger(\hat{a}_{H_{12}}^\dagger - \hat{a}_{V_{12}}^\dagger) + \alpha_3\hat{a}_{V_{1'}}^\dagger(\hat{a}_{H_{12}}^\dagger - \hat{a}_{V_{12}}^\dagger) + \alpha_4\hat{a}_{V_{1''}}^\dagger(\hat{a}_{H_{12}}^\dagger + \hat{a}_{V_{12}}^\dagger)]|vac.\rangle. \quad (25)$$

(ii) When the outing photons emitted from spatial mode pairs  $(10, 12)$  and  $(1'', 12)$ , the state  $|\chi_{9,1',12}\rangle_1$  and  $|\chi_{10,1'',12}\rangle_1$  both become

$$|\chi_{10,1'',12}^+\rangle_2 = \frac{1}{8\sqrt{2}} [\alpha_1\hat{a}_{H_{10}}^\dagger(\hat{a}_{H_{12}}^\dagger + \hat{a}_{V_{12}}^\dagger) + \alpha_2\hat{a}_{H_{10}}^\dagger(\hat{a}_{H_{12}}^\dagger - \hat{a}_{V_{12}}^\dagger) + \alpha_3\hat{a}_{V_{1''}}^\dagger(\hat{a}_{H_{12}}^\dagger - \hat{a}_{V_{12}}^\dagger) + \alpha_4\hat{a}_{V_{1'}}^\dagger(\hat{a}_{H_{12}}^\dagger + \hat{a}_{V_{12}}^\dagger)]|vac.\rangle. \quad (26)$$

(iii) When the outing photons emitted from spatial mode pairs  $(9, 11)$  and  $(1'', 11)$ , the state  $|\chi_{9,1',11}\rangle_1$  and  $|\chi_{10,1'',11}\rangle_1$  both become

$$|\chi_{9,1',11}^-\rangle_2 = \frac{1}{8\sqrt{2}} [\alpha_1\hat{a}_{H_9}^\dagger(\hat{a}_{H_{11}}^\dagger + \hat{a}_{V_{11}}^\dagger) + \alpha_2\hat{a}_{H_9}^\dagger(\hat{a}_{H_{11}}^\dagger - \hat{a}_{V_{11}}^\dagger) - \alpha_3\hat{a}_{V_{1'}}^\dagger(\hat{a}_{H_{11}}^\dagger - \hat{a}_{V_{11}}^\dagger) - \alpha_4\hat{a}_{V_{1''}}^\dagger(\hat{a}_{H_{11}}^\dagger + \hat{a}_{V_{11}}^\dagger)]|vac.\rangle. \quad (27)$$

(iv) When the outing photons emitted from spatial mode pairs  $(10, 11)$  and  $(1'', 11)$ , the state  $|\chi_{9,1',12}\rangle_1$  and  $|\chi_{10,1'',12}\rangle_1$  both become

$$|\chi_{10,1'',11}^-\rangle_2 = \frac{1}{8\sqrt{2}} [\alpha_1 \hat{a}_{H_{10}}^\dagger (\hat{a}_{H_{11}}^\dagger + \hat{a}_{V_{11}}^\dagger) + \alpha_2 \hat{a}_{H_{10}}^\dagger (\hat{a}_{H_{11}}^\dagger - \hat{a}_{V_{11}}^\dagger) - \alpha_3 \hat{a}_{V_{1''}}^\dagger (\hat{a}_{H_{11}}^\dagger - \hat{a}_{V_{11}}^\dagger) - \alpha_4 \hat{a}_{V_{1''}}^\dagger (\hat{a}_{H_{11}}^\dagger + \hat{a}_{V_{11}}^\dagger)] |\text{vac.}\rangle. \quad (28)$$

Fourth, as shown in Fig. 5, PBS<sub>2</sub> leads the photons in modes 9 (i.e.,  $\hat{a}_{H_9}^\dagger |\text{vac.}\rangle$ ) and  $1'$  (i.e.,  $\hat{a}_{V_1'}^\dagger |\text{vac.}\rangle$ ) into one output mode, and combines the photons in modes 10 (i.e.,  $\hat{a}_{H_{10}}^\dagger |\text{vac.}\rangle$ ) and  $1''$  (i.e.,  $\hat{a}_{V_{1''}}^\dagger |\text{vac.}\rangle$ ) into one output mode. After PBS<sub>2</sub> and HWP<sup>22.5°</sup>, (i) when the photons emitted from outport pair  $(9, 12)$ , we obtain the two-fold output state

$$|\chi_{9,12}^+\rangle_3 = \frac{1}{8} (\alpha_1 \hat{a}_{H_9}^\dagger \hat{a}_{H_{12}}^\dagger + \alpha_2 \hat{a}_{H_9}^\dagger \hat{a}_{V_{12}}^\dagger + \alpha_3 \hat{a}_{V_9}^\dagger \hat{a}_{V_{12}}^\dagger + \alpha_4 \hat{a}_{V_9}^\dagger \hat{a}_{H_{12}}^\dagger) |\text{vac.}\rangle. \quad (29)$$

The CNOT gate is completed.

(ii) When the photons emitted from outport pair  $(10, 12)$ , we obtain the two-fold output state

$$|\chi_{10,12}^+\rangle_3 = \frac{1}{8} (\alpha_1 \hat{a}_{H_{10}}^\dagger \hat{a}_{H_{12}}^\dagger + \alpha_2 \hat{a}_{H_{10}}^\dagger \hat{a}_{V_{12}}^\dagger + \alpha_3 \hat{a}_{V_{10}}^\dagger \hat{a}_{V_{12}}^\dagger + \alpha_4 \hat{a}_{V_{10}}^\dagger \hat{a}_{H_{12}}^\dagger) |\text{vac.}\rangle. \quad (30)$$

The CNOT gate is completed.

(iii) When the photons emitted from outport pair  $(9, 11)$ , we obtain the two-fold output state

$$|\chi_{9,11}^-\rangle_3 = \frac{1}{8} (\alpha_1 \hat{a}_{H_9}^\dagger \hat{a}_{H_{11}}^\dagger + \alpha_2 \hat{a}_{H_9}^\dagger \hat{a}_{V_{11}}^\dagger - \alpha_3 \hat{a}_{V_9}^\dagger \hat{a}_{V_{11}}^\dagger - \alpha_4 \hat{a}_{V_9}^\dagger \hat{a}_{H_{11}}^\dagger) |\text{vac.}\rangle. \quad (31)$$

And then an HWP<sup>0°</sup> is set in the output mode 9 to complete the CNOT gate.

(iv) When the photons emitted from outport pair  $(10, 11)$ , we obtain the two-fold output state

$$|\chi_{10,11}^-\rangle_3 = \frac{1}{8} (\alpha_1 \hat{a}_{H_{10}}^\dagger \hat{a}_{H_{11}}^\dagger + \alpha_2 \hat{a}_{H_{10}}^\dagger \hat{a}_{V_{11}}^\dagger - \alpha_3 \hat{a}_{V_{10}}^\dagger \hat{a}_{V_{11}}^\dagger - \alpha_4 \hat{a}_{V_{10}}^\dagger \hat{a}_{H_{11}}^\dagger) |\text{vac.}\rangle. \quad (32)$$

And then an HWP<sup>0°</sup> is set in the output mode 10 to complete the CNOT gate.

Based on above orthogonal two-fold states  $|\chi_{9,12}^+\rangle_3$ ,  $|\chi_{10,12}^+\rangle_3$ ,  $|\chi_{9,11}^-\rangle_3$ , and  $|\chi_{10,11}^-\rangle_3$ , one can find that after the feed-forward operations are only applied to the rightmost P-SWAP gate, an optical post-selection CNOT gate can be completed with a success probability of  $8 \times 1/64 = 1/8$ . Remarkably, additional entangled photon pairs or single photons are necessary for previous schemes [59–61, 63, 64], but are not required for our CNOT gate. In addition, the success probability of the gate is improved on the results without an auxiliary photon [65–67].

### 3.3 Implementation of a Toffoli gate with linear optics

We propose the implementation of a Toffoli gate based on the designed P-SWAP and CNOT gates. As shown in Fig. 6, three photons are injected into modes 1, 2, and 3, simultaneously, the initial state is given by

$$|\Xi_0\rangle = (\alpha_1 \hat{a}_{H_1}^\dagger \hat{a}_{H_2}^\dagger \hat{a}_{H_3}^\dagger + \alpha_2 \hat{a}_{H_1}^\dagger \hat{a}_{H_2}^\dagger \hat{a}_{V_3}^\dagger + \alpha_3 \hat{a}_{H_1}^\dagger \hat{a}_{V_2}^\dagger \hat{a}_{H_3}^\dagger + \alpha_4 \hat{a}_{H_1}^\dagger \hat{a}_{V_2}^\dagger \hat{a}_{V_3}^\dagger + \alpha_5 \hat{a}_{V_1}^\dagger \hat{a}_{H_2}^\dagger \hat{a}_{H_3}^\dagger + \alpha_6 \hat{a}_{V_1}^\dagger \hat{a}_{H_2}^\dagger \hat{a}_{V_3}^\dagger + \alpha_7 \hat{a}_{V_1}^\dagger \hat{a}_{V_2}^\dagger \hat{a}_{H_3}^\dagger + \alpha_8 \hat{a}_{V_1}^\dagger \hat{a}_{V_2}^\dagger \hat{a}_{V_3}^\dagger) |\text{vac.}\rangle. \quad (33)$$

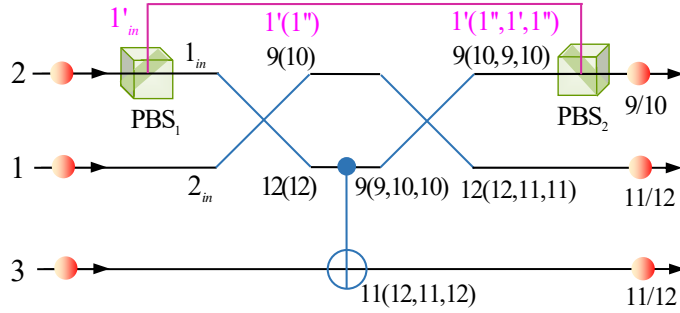


Figure 6: Optical implementation of a three-photon Toffoli gate.

First, after photons go through the  $\text{PBS}_1$  and the leftmost P-SWAP gate, when the outing photons emitted from path pairs  $(9, 12)$  and  $(1', 12)$ , or  $(10, 12)$  and  $(1'', 12)$ , we can obtain two desired states,

$$|\Xi_{1a}\rangle = \frac{1}{2\sqrt{2}} (\alpha_1 \hat{a}_{H_{12}}^\dagger \hat{a}_{H_9}^\dagger \hat{a}_{H_3}^\dagger + \alpha_2 \hat{a}_{H_{12}}^\dagger \hat{a}_{H_9}^\dagger \hat{a}_{V_3}^\dagger + \alpha_3 \hat{a}_{H_{12}}^\dagger \hat{a}_{V_1'}^\dagger \hat{a}_{H_3}^\dagger + \alpha_4 \hat{a}_{H_{12}}^\dagger \hat{a}_{V_1'}^\dagger \hat{a}_{V_3}^\dagger + \alpha_5 \hat{a}_{H_{12}}^\dagger \hat{a}_{V_9}^\dagger \hat{a}_{H_3}^\dagger + \alpha_6 \hat{a}_{H_{12}}^\dagger \hat{a}_{V_9}^\dagger \hat{a}_{V_3}^\dagger + \alpha_7 \hat{a}_{V_{12}}^\dagger \hat{a}_{V_1'}^\dagger \hat{a}_{H_3}^\dagger + \alpha_8 \hat{a}_{V_{12}}^\dagger \hat{a}_{V_1'}^\dagger \hat{a}_{V_3}^\dagger) |\text{vac.}\rangle, \quad (34)$$

$$|\Xi_{1b}\rangle = \frac{1}{2\sqrt{2}} (\alpha_1 \hat{a}_{H_{12}}^\dagger \hat{a}_{H_{10}}^\dagger \hat{a}_{H_3}^\dagger + \alpha_2 \hat{a}_{H_{12}}^\dagger \hat{a}_{H_{10}}^\dagger \hat{a}_{V_3}^\dagger + \alpha_3 \hat{a}_{H_{12}}^\dagger \hat{a}_{V_{1''}}^\dagger \hat{a}_{H_3}^\dagger + \alpha_4 \hat{a}_{H_{12}}^\dagger \hat{a}_{V_{1''}}^\dagger \hat{a}_{V_3}^\dagger + \alpha_5 \hat{a}_{H_{12}}^\dagger \hat{a}_{V_{10}}^\dagger \hat{a}_{H_3}^\dagger + \alpha_6 \hat{a}_{H_{12}}^\dagger \hat{a}_{V_{10}}^\dagger \hat{a}_{V_3}^\dagger + \alpha_7 \hat{a}_{V_{12}}^\dagger \hat{a}_{V_{1''}}^\dagger \hat{a}_{H_3}^\dagger + \alpha_8 \hat{a}_{V_{12}}^\dagger \hat{a}_{V_{1''}}^\dagger \hat{a}_{V_3}^\dagger) |\text{vac.}\rangle. \quad (35)$$

Second, the states described by Eqs. (34) and (35) are considered as the inputs for the next CNOT gate acting on photon 1 and photon 3. When the outing photons emitted from path pairs  $(9, 11)$ ,  $(9, 12)$ ,  $(10, 11)$ , or  $(10, 12)$ , which can yield 16 desired states  $|\Xi_{i,9,k}\rangle_1$  (two-fold) and  $|\Xi_{i,10,k}\rangle_1$  (two-fold). Here,  $|\Xi_{i,9,k}\rangle_1$  and  $|\Xi_{i,10,k}\rangle_1$  with  $i \in \{9, 10\}$  and  $k \in \{11, 12\}$  are described by

$$|\Xi_{i,9,k}\rangle_1 = \frac{1}{16\sqrt{2}} (\alpha_1 \hat{a}_{H_i}^\dagger \hat{a}_{H_9}^\dagger \hat{a}_{H_k}^\dagger + \alpha_2 \hat{a}_{H_i}^\dagger \hat{a}_{H_9}^\dagger \hat{a}_{V_k}^\dagger + \alpha_3 \hat{a}_{H_i}^\dagger \hat{a}_{V_1'}^\dagger \hat{a}_{H_k}^\dagger + \alpha_4 \hat{a}_{H_i}^\dagger \hat{a}_{V_1'}^\dagger \hat{a}_{V_k}^\dagger + \alpha_5 \hat{a}_{H_i}^\dagger \hat{a}_{V_9}^\dagger \hat{a}_{H_k}^\dagger + \alpha_6 \hat{a}_{H_i}^\dagger \hat{a}_{V_9}^\dagger \hat{a}_{V_k}^\dagger + \alpha_7 \hat{a}_{V_i}^\dagger \hat{a}_{V_1'}^\dagger \hat{a}_{V_k}^\dagger + \alpha_8 \hat{a}_{V_i}^\dagger \hat{a}_{V_1'}^\dagger \hat{a}_{H_k}^\dagger) |\text{vac.}\rangle, \quad (36)$$

$$|\Xi_{i,10,k}\rangle_1 = \frac{1}{16\sqrt{2}} (\alpha_1 \hat{a}_{H_i}^\dagger \hat{a}_{H_{10}}^\dagger \hat{a}_{H_k}^\dagger + \alpha_2 \hat{a}_{H_i}^\dagger \hat{a}_{H_{10}}^\dagger \hat{a}_{V_k}^\dagger + \alpha_3 \hat{a}_{H_i}^\dagger \hat{a}_{V_{1''}}^\dagger \hat{a}_{H_k}^\dagger + \alpha_4 \hat{a}_{H_i}^\dagger \hat{a}_{V_{1''}}^\dagger \hat{a}_{V_k}^\dagger + \alpha_5 \hat{a}_{H_i}^\dagger \hat{a}_{V_{10}}^\dagger \hat{a}_{H_k}^\dagger + \alpha_6 \hat{a}_{H_i}^\dagger \hat{a}_{V_{10}}^\dagger \hat{a}_{V_k}^\dagger + \alpha_7 \hat{a}_{V_i}^\dagger \hat{a}_{V_{1''}}^\dagger \hat{a}_{V_k}^\dagger + \alpha_8 \hat{a}_{V_i}^\dagger \hat{a}_{V_{1''}}^\dagger \hat{a}_{H_k}^\dagger) |\text{vac.}\rangle. \quad (37)$$

Third, above 16 states are considered as inputs for the rightmost P-SWAP gate acting on photon 1 and photon 2. When the photon emitted from path pairs  $(9, 12)$  and  $(1', 12)$ , or  $(9, 11)$  and  $(1', 11)$ , or  $(10, 12)$  and  $(1'', 12)$ , or  $(10, 11)$  and  $(1'', 11)$ , we can obtain 64 desired states  $|\Xi_{12,9,k}^+\rangle_2$ ,  $|\Xi_{12,10,k}^+\rangle_2$ ,  $|\Xi_{11,9,k}^-\rangle_2$  and  $|\Xi_{11,10,k}^-\rangle_2$ . Here, eight-fold states  $|\Xi_{12,9,k}^+\rangle_2$ ,

$|\Xi_{12,10,k}^+\rangle_2$ ,  $|\Xi_{11,9,k}^-\rangle_2$ , and  $|\Xi_{11,10,k}^-\rangle_2$  with  $k \in \{11, 12\}$  are described by

$$|\Xi_{12,9,k}^+\rangle_2 = \frac{1}{64} [\alpha_1 \hat{a}_{H_{12}}^\dagger \hat{a}_{H_9}^\dagger \hat{a}_{H_k}^\dagger + \alpha_2 \hat{a}_{H_{12}}^\dagger \hat{a}_{H_9}^\dagger \hat{a}_{V_k}^\dagger + \alpha_3 \hat{a}_{H_{12}}^\dagger \hat{a}_{V_{1'}}^\dagger \hat{a}_{H_k}^\dagger + \alpha_4 \hat{a}_{H_{12}}^\dagger \hat{a}_{V_{1'}}^\dagger \hat{a}_{V_k}^\dagger + \alpha_5 \hat{a}_{V_{12}}^\dagger \hat{a}_{H_9}^\dagger \hat{a}_{H_k}^\dagger + \alpha_6 \hat{a}_{V_{12}}^\dagger \hat{a}_{H_9}^\dagger \hat{a}_{V_k}^\dagger + \alpha_7 \hat{a}_{V_{12}}^\dagger \hat{a}_{V_{1'}}^\dagger \hat{a}_{V_k}^\dagger + \alpha_8 \hat{a}_{V_{12}}^\dagger \hat{a}_{V_{1'}}^\dagger \hat{a}_{H_k}^\dagger] |\text{vac.}\rangle, \quad (38)$$

$$|\Xi_{12,10,k}^+\rangle_2 = \frac{1}{64} [\alpha_1 \hat{a}_{H_{12}}^\dagger \hat{a}_{H_{10}}^\dagger \hat{a}_{H_k}^\dagger + \alpha_2 \hat{a}_{H_{12}}^\dagger \hat{a}_{H_{10}}^\dagger \hat{a}_{V_k}^\dagger + \alpha_3 \hat{a}_{H_{12}}^\dagger \hat{a}_{V_{1''}}^\dagger \hat{a}_{H_k}^\dagger + \alpha_4 \hat{a}_{H_{12}}^\dagger \hat{a}_{V_{1''}}^\dagger \hat{a}_{V_k}^\dagger + \alpha_5 \hat{a}_{V_{12}}^\dagger \hat{a}_{H_{10}}^\dagger \hat{a}_{H_k}^\dagger + \alpha_6 \hat{a}_{V_{12}}^\dagger \hat{a}_{H_{10}}^\dagger \hat{a}_{V_k}^\dagger + \alpha_7 \hat{a}_{V_{12}}^\dagger \hat{a}_{V_{1''}}^\dagger \hat{a}_{V_k}^\dagger + \alpha_8 \hat{a}_{V_{12}}^\dagger \hat{a}_{V_{1''}}^\dagger \hat{a}_{H_k}^\dagger] |\text{vac.}\rangle, \quad (39)$$

$$|\Xi_{11,9,k}^-\rangle_2 = \frac{1}{64} [\alpha_1 \hat{a}_{H_{11}}^\dagger \hat{a}_{H_9}^\dagger \hat{a}_{H_k}^\dagger + \alpha_2 \hat{a}_{H_{11}}^\dagger \hat{a}_{H_9}^\dagger \hat{a}_{V_k}^\dagger - \alpha_3 \hat{a}_{H_{11}}^\dagger \hat{a}_{V_{1'}}^\dagger \hat{a}_{H_k}^\dagger - \alpha_4 \hat{a}_{H_{11}}^\dagger \hat{a}_{V_{1'}}^\dagger \hat{a}_{V_k}^\dagger + \alpha_5 \hat{a}_{V_{11}}^\dagger \hat{a}_{H_9}^\dagger \hat{a}_{H_k}^\dagger + \alpha_6 \hat{a}_{V_{11}}^\dagger \hat{a}_{H_9}^\dagger \hat{a}_{V_k}^\dagger - \alpha_7 \hat{a}_{V_{11}}^\dagger \hat{a}_{V_{1'}}^\dagger \hat{a}_{H_k}^\dagger - \alpha_8 \hat{a}_{V_{11}}^\dagger \hat{a}_{V_{1'}}^\dagger \hat{a}_{V_k}^\dagger] |\text{vac.}\rangle, \quad (40)$$

$$|\Xi_{11,10,k}^-\rangle_2 = \frac{1}{64} [\alpha_1 \hat{a}_{H_{11}}^\dagger \hat{a}_{H_{10}}^\dagger \hat{a}_{H_k}^\dagger + \alpha_2 \hat{a}_{H_{11}}^\dagger \hat{a}_{H_{10}}^\dagger \hat{a}_{V_k}^\dagger - \alpha_3 \hat{a}_{H_{11}}^\dagger \hat{a}_{V_{1''}}^\dagger \hat{a}_{H_k}^\dagger - \alpha_4 \hat{a}_{H_{11}}^\dagger \hat{a}_{V_{1''}}^\dagger \hat{a}_{V_k}^\dagger + \alpha_5 \hat{a}_{V_{11}}^\dagger \hat{a}_{H_{10}}^\dagger \hat{a}_{H_k}^\dagger + \alpha_6 \hat{a}_{V_{11}}^\dagger \hat{a}_{H_{10}}^\dagger \hat{a}_{V_k}^\dagger - \alpha_7 \hat{a}_{V_{11}}^\dagger \hat{a}_{V_{1''}}^\dagger \hat{a}_{V_k}^\dagger - \alpha_8 \hat{a}_{V_{11}}^\dagger \hat{a}_{V_{1''}}^\dagger \hat{a}_{H_k}^\dagger] |\text{vac.}\rangle. \quad (41)$$

Finally, as shown in Fig. 6, the photons emitted from modes 9 (i.e.,  $\hat{a}_{H_9}^\dagger |\text{vac.}\rangle$ ) and 1' (i.e.,  $\hat{a}_{V_{1'}}^\dagger |\text{vac.}\rangle$ ) are combined into the same output mode by PBS<sub>2</sub>. The photons emitted from modes 10 (i.e.,  $\hat{a}_{H_{10}}^\dagger |\text{vac.}\rangle$ ) and 1'' ( $\hat{a}_{V_{1''}}^\dagger |\text{vac.}\rangle$ ) are also leaded to the same output mode by PBS<sub>2</sub>. Therefore, after PBS<sub>2</sub>, (i) when the photons emitted from outport pairs (12, 9, k) with  $k \in \{11, 12\}$ , simultaneously, we obtain the eight-fold state

$$|\Xi_{12,9,k}^+\rangle_3 = \frac{1}{64} [\alpha_1 \hat{a}_{H_{12}}^\dagger \hat{a}_{H_9}^\dagger \hat{a}_{H_k}^\dagger + \alpha_2 \hat{a}_{H_{12}}^\dagger \hat{a}_{H_9}^\dagger \hat{a}_{V_k}^\dagger + \alpha_3 \hat{a}_{H_{12}}^\dagger \hat{a}_{V_9}^\dagger \hat{a}_{H_k}^\dagger + \alpha_4 \hat{a}_{H_{12}}^\dagger \hat{a}_{V_9}^\dagger \hat{a}_{V_k}^\dagger + \alpha_5 \hat{a}_{V_{12}}^\dagger \hat{a}_{H_9}^\dagger \hat{a}_{H_k}^\dagger + \alpha_6 \hat{a}_{V_{12}}^\dagger \hat{a}_{H_9}^\dagger \hat{a}_{V_k}^\dagger + \alpha_7 \hat{a}_{V_{12}}^\dagger \hat{a}_{V_9}^\dagger \hat{a}_{V_k}^\dagger + \alpha_8 \hat{a}_{V_{12}}^\dagger \hat{a}_{V_9}^\dagger \hat{a}_{H_k}^\dagger] |\text{vac.}\rangle. \quad (42)$$

The three-photon Toffoli gate is completed.

(ii) When the photons emitted from outport pairs  $(12, 10, k)$  with  $k \in \{11, 12\}$ , simultaneously, we obtain the eight-fold state

$$|\Xi_{12,10,k}^+\rangle_3 = \frac{1}{64} [\alpha_1 \hat{a}_{H_{12}}^\dagger \hat{a}_{H_{10}}^\dagger \hat{a}_{H_k}^\dagger + \alpha_2 \hat{a}_{H_{12}}^\dagger \hat{a}_{H_{10}}^\dagger \hat{a}_{V_k}^\dagger + \alpha_3 \hat{a}_{H_{12}}^\dagger \hat{a}_{V_{10}}^\dagger \hat{a}_{H_k}^\dagger + \alpha_4 \hat{a}_{H_{12}}^\dagger \hat{a}_{V_{10}}^\dagger \hat{a}_{V_k}^\dagger + \alpha_5 \hat{a}_{V_{12}}^\dagger \hat{a}_{H_{10}}^\dagger \hat{a}_{H_k}^\dagger + \alpha_6 \hat{a}_{V_{12}}^\dagger \hat{a}_{H_{10}}^\dagger \hat{a}_{V_k}^\dagger + \alpha_7 \hat{a}_{V_{12}}^\dagger \hat{a}_{V_{10}}^\dagger \hat{a}_{V_k}^\dagger + \alpha_8 \hat{a}_{V_{12}}^\dagger \hat{a}_{V_{10}}^\dagger \hat{a}_{H_k}^\dagger] |\text{vac.}\rangle. \quad (43)$$

The three-photon Toffoli gate is also completed.

(iii) When the photons emitted from outport pairs  $(11, 9, k)$  with  $k \in \{11, 12\}$ , simultaneously, we obtain the eight-fold state

$$|\Xi_{11,9,k}^-\rangle_3 = \frac{1}{64} [\alpha_1 \hat{a}_{H_{11}}^\dagger \hat{a}_{H_9}^\dagger \hat{a}_{H_k}^\dagger + \alpha_2 \hat{a}_{H_{11}}^\dagger \hat{a}_{H_9}^\dagger \hat{a}_{V_k}^\dagger - \alpha_3 \hat{a}_{H_{11}}^\dagger \hat{a}_{V_9}^\dagger \hat{a}_{H_k}^\dagger - \alpha_4 \hat{a}_{H_{11}}^\dagger \hat{a}_{V_9}^\dagger \hat{a}_{V_k}^\dagger + \alpha_5 \hat{a}_{V_{11}}^\dagger \hat{a}_{H_9}^\dagger \hat{a}_{H_k}^\dagger + \alpha_6 \hat{a}_{V_{11}}^\dagger \hat{a}_{H_9}^\dagger \hat{a}_{V_k}^\dagger - \alpha_7 \hat{a}_{V_{11}}^\dagger \hat{a}_{V_9}^\dagger \hat{a}_{H_k}^\dagger - \alpha_8 \hat{a}_{V_{11}}^\dagger \hat{a}_{V_9}^\dagger \hat{a}_{V_k}^\dagger] |\text{vac.}\rangle. \quad (44)$$

And then an HWP ${}^{0^\circ}$  is set in the output mode 9 to complete the three-photon Toffoli gate.

(iv) When the photons emitted from outport pairs  $(11, 10, k)$  with  $k \in \{11, 12\}$ , simultaneously, we obtain the eight-fold state

$$|\Xi_{11,10,k}^-\rangle_3 = \frac{1}{64} [\alpha_1 \hat{a}_{H_{11}}^\dagger \hat{a}_{H_{10}}^\dagger \hat{a}_{H_k}^\dagger + \alpha_2 \hat{a}_{H_{11}}^\dagger \hat{a}_{H_{10}}^\dagger \hat{a}_{V_k}^\dagger - \alpha_3 \hat{a}_{H_{11}}^\dagger \hat{a}_{V_{10}}^\dagger \hat{a}_{H_k}^\dagger - \alpha_4 \hat{a}_{H_{11}}^\dagger \hat{a}_{V_{10}}^\dagger \hat{a}_{V_k}^\dagger + \alpha_5 \hat{a}_{V_{11}}^\dagger \hat{a}_{H_{10}}^\dagger \hat{a}_{H_k}^\dagger + \alpha_6 \hat{a}_{V_{11}}^\dagger \hat{a}_{H_{10}}^\dagger \hat{a}_{V_k}^\dagger - \alpha_7 \hat{a}_{V_{11}}^\dagger \hat{a}_{V_{10}}^\dagger \hat{a}_{V_k}^\dagger - \alpha_8 \hat{a}_{V_{11}}^\dagger \hat{a}_{V_{10}}^\dagger \hat{a}_{H_k}^\dagger] |\text{vac.}\rangle. \quad (45)$$

And then an HWP ${}^{0^\circ}$  is set in the output mode 10 to complete the three-photon Toffoli gate.

Based on above orthogonal eight-fold states described by Eqs. (42-45), one can find that our proposal can be achieved with a higher success probability ( $64 \times 1/64^2 = 1/64$ ) than the simplified CNOT-based one ( $1/72$ ) [20, 21] and the one without a decomposition-based approach ( $1/133$ ) [58]. In addition, optical single-qudit operation ensembles  $X_a, X_b, \dots, X_n$  can be achieved by employing a sequence of PBSs, and the linear optical  $n$ -control-photon Toffoli gate can be implemented in principle (see Fig. 7).

## 4 Discussion and Conclusion

The optimal cost of a Toffoli gate is six CNOT gates using the standard decomposition-based approach in qubit system [47]. The theoretical lower bound of a Toffoli gate is five two-qubit gates in qubit system [48]. Ralph *et al.* [20] first reduced the cost of a Toffoli gate to three qubit-qudit CNOT gates by introducing a qutrit. Using the same idea as the works in Refs. [20, 21], we designed an alternative the quantum circuit to implement the Toffoli gate with

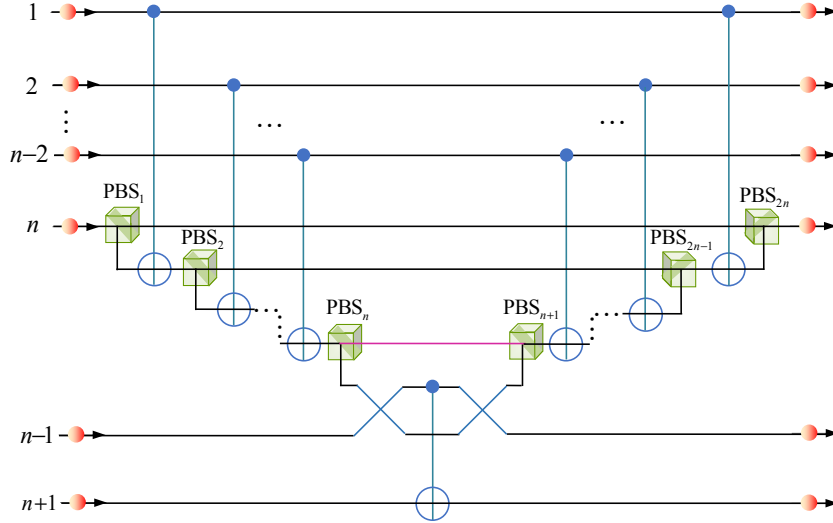


Figure 7: Implementation of an  $(n + 1)$ -photon Toffoli gate.

a higher success probability based on the P-SWAP gates, which required the same number of qubit-qudit gates as the protocols in Refs. [20, 21]. The required qubit-qudit entangled gates are all nearest neighbors in our construction of the three-qubit Toffoli gate. Note that the nearest-neighbor quantum gate where each qubit interacts only with its nearest neighbors requires less resource overhead than the long-range one. For example, a long-range CNOT gate acting on the first qubit and the third qubit is constructed by four nearest-neighbor CNOT gates [68]. In addition,  $(2n - 1)$  qubit-qudit gates and  $(2n - 2)$  single-qudit gates can simulate an  $n$ -control-qubit Toffoli gate in higher-dimensional spaces.

Linear optics has inherent probability characteristics for the implementation of controlled quantum gates. With the help of an additional entangled photon pair [60, 63] or a single photon [64], optical CNOT gate with a success probability of  $1/4$  or  $1/8$  can be realistically implemented. Without auxiliary photons, CNOT gate with a success probability of  $1/9$  has been experimentally demonstrated in linear optics [65–67]. Remarkably, the success probability of our P-SWAP-based CNOT gate is enhanced to  $1/8$  without additional photons. Moreover, the success probability of our P-SWAP-based Toffoli gate ( $1/64$ ) is higher than the CNOT-based protocols ( $1/72$ ) [20, 21] and it is also higher than the no-decomposition-based one ( $1/133$ ) [58].

The multi-level system is essential to realize our schemes. In optical system, we can encode polarization DOF of photons as two computational qubits and spatial-mode DOF as the qudit (extra level). We can also encode these levels on orbital angular momentum of photons. Besides, diamond nitrogen-vacancy defect center [69, 70] and superconducting system [71, 72] can also provide available multiple levels to implement the universal quantum gates due to their long coherence time and flexible manipulation.

In summary, by introducing higher-dimensional spaces, we proposed simplified CNOT and Toffoli gates. A three-qubit Toffoli gate can be simulated with two P-SWAP, one CNOT, and two single-qutrit gates.  $(2n - 1)$  qubit-qudit gates and  $(2n - 2)$  single-qudit gates are sufficient for constructing an  $n$ -control-qubit Toffoli gate. Following the simplified synthesis, as a feasible example, linear optics architectures for implementing CNOT and Toffoli gates were designed with a higher success probability.

## Acknowledgments

This work is supported by the National Natural Science Foundation of China under Grant No. 11604012, the Fundamental Research Funds for the Central Universities under Grants No. FRF-TP-19-011A3 and No. 230201506500024, and a grant from the China Scholarship Council. L.-C.K. is supported by the Ministry of Education and the National Research Foundation Singapore.

## References

- [1] A. Barenco, C. H. Bennett, R. Cleve, D. P. DiVincenzo, N. Margolus, P. Shor, T. Sleator, J. A. Smolin and H. Weinfurter, *Elementary gates for quantum computation*, Physical Review A **52**, 3457 (1995), doi:10.1103/PhysRevA.52.3457.
- [2] L. K. Grover, *Quantum mechanics helps in searching for a needle in a haystack*, doi:10.1103/PhysRevLett.79.325 (1997).
- [3] P. W. Shor, *Polynomial-time algorithms for prime factorization and discrete logarithms on a quantum computer*, SIAM Review **41**, 303 (1999), doi:10.1137/S0036144598347011.
- [4] C. Figgatt, D. Maslov, K. Landsman, N. M. Linke, S. Debnath and C. Monroe, *Complete 3-qubit Grover search on a programmable quantum computer*, Nature Communications **8**, 1918 (2017), doi:10.1038/s41467-017-01904-7.
- [5] Y. Nam, Y. Su and D. Maslov, *Approximate quantum Fourier transform with  $o(n \log(n))$  T gates*, npj Quantum Information **6**, 26 (2020), doi:10.1038/s41534-020-0257-5.
- [6] N. Gisin, G. Ribordy, W. Tittel and H. Zbinden, *Quantum cryptography*, Reviews of Modern Physics **74**, 145 (2002), doi:10.1103/RevModPhys.74.145.
- [7] M. A. Nielsen and I. L. Chuang, *Quantum Computation and Quantum Information: 10th Anniversary Edition*, Cambridge University Press, doi:10.1017/CBO9780511976667 (2010).
- [8] B. P. Lanyon, M. Barbieri, M. P. Almeida and A. G. White, *Experimental quantum computing without entanglement*, Physical Review Letters **101**, 200501 (2008), doi:10.1103/PhysRevLett.101.200501.
- [9] V. V. Shende, I. L. Markov and S. S. Bullock, *Minimal universal two-qubit controlled-NOT-based circuits*, Physical Review A **69**, 062321 (2004), doi:10.1103/PhysRevA.69.062321.
- [10] N. Khaneja and S. J. Glaser, *Cartan decomposition of  $SU(2^n)$  and control of spin systems*, Chemical Physics **267**, 11 (2001), doi:10.1016/S0301-0104(01)00318-4.
- [11] M. Möttönen, J. J. Vartiainen, V. Bergholm and M. M. Salomaa, *Quantum circuits for general multiqubit gates*, Physical Review Letters **93**, 130502 (2004), doi:10.1103/PhysRevLett.93.130502.

- [12] S. S. Bullock and G. K. Brennen, *Canonical decompositions of n-qubit quantum computations and concurrence*, Journal of Mathematical Physics **45**, 2447 (2004), doi:10.1063/1.17237012.
- [13] V. V. Shende, S. S. Bullock and I. L. Markov, *Synthesis of quantum-logic circuits*, IEEE Transactions on Computer-Aided Design of Integrated Circuits and Systems **25**, 1000 (2006), doi:10.1109/TCAD.2005.855930.
- [14] D. D'Alessandro and F. Albertini, *Quantum symmetries and Cartan decompositions in arbitrary dimensions*, Journal of Physics A: Mathematical and Theoretical **40**, 2439 (2007), doi:10.1088/1751-8113/40/10/013.
- [15] Y. M. Di and H. R. Wei, *Synthesis of multivalued quantum logic circuits by elementary gates*, Physical Review A **87**, 012325 (2013), doi:10.1103/PhysRevA.87.012325.
- [16] R. Iten, R. Colbeck, I. Kukuljan, J. Home and M. Christandl, *Quantum circuits for isometries*, Physical Review A **93**, 032318 (2016), doi:10.1103/PhysRevA.93.032318.
- [17] F. Vatan and C. Williams, *Optimal quantum circuits for general two-qubit gates*, Physical Review A **69**, 032315 (2004), doi:10.1103/PhysRevA.69.032315.
- [18] G. Vidal and C. M. Dawson, *Universal quantum circuit for two-qubit transformations with three controlled-NOT gates*, Physical Review A **69**, 010301(R) (2004), doi:10.1103/PhysRevA.69.010301.
- [19] V. V. Shende, S. S. Bullock and I. L. Markov, *Recognizing small-circuit structure in two-qubit operators*, Physical Review A **70**, 012310 (2004), doi:10.1103/PhysRevA.70.012310.
- [20] T. C. Ralph, K. J. Resch and A. Gilchrist, *Efficient Toffoli gates using qudits*, Physical Review A **75**, 022313 (2007), doi:10.1103/PhysRevA.75.022313.
- [21] B. P. Lanyon, M. Barbieri, M. P. Almeida, T. Jennewein, T. C. Ralph, K. J. Resch, G. J. Pryde, J. L. O'brien, A. Gilchrist and A. G. White, *Simplifying quantum logic using higher-dimensional Hilbert spaces*, Nature Physics **5**, 134 (2009), doi:10.1038/nphys1150.
- [22] A. Fedorov, L. Steffen, M. Baur, M. P. da Silva and A. Wallraff, *Implementation of a Toffoli gate with superconducting circuits*, Nature **481**, 170 (2012), doi:10.1038/nature10713.
- [23] K. Liu, W. D. Li, W. Z. Zhang, P. Shi, C. N. Ren and Y. J. Gu, *Optimizing quantum circuits using higher-dimensional Hilbert spaces*, Acta Physica Sinica **61**, 120301 (2012), doi:10.7498/aps.61.120301.
- [24] W. D. Li, Y. J. Gu, K. Liu, Y. H. Lee and Y. Z. Zhang, *Efficient universal quantum computation with auxiliary Hilbert space*, Physical Review A **88**, 034303 (2013), doi:10.1103/PhysRevA.88.034303.
- [25] W. Q. Liu and H. R. Wei, *Optimal synthesis of the Fredkin gate in a multilevel system*, New Journal of Physics **22**, 063026 (2020), doi:10.1088/1367-2630/ab8e13.
- [26] W. Q. Liu, H. R. Wei and L. C. Kwek, *Low-cost Fredkin gate with auxiliary space*, Physical Review Applied **14**, 054057 (2020), doi:10.1103/PhysRevApplied.14.054057.

- [27] A. Sawicki and K. Karnas, *Criteria for universality of quantum gates*, Physical Review A **95**, 062303 (2017), doi:10.1103/PhysRevA.95.062303.
- [28] A. Sawicki and K. Karnas, *Universality of single-qudit gates*, Annales Henri Poincaré **18**, 3515 (2017), doi:10.1007/s00023-017-0604-z.
- [29] K. Lemr, K. Bartkiewicz, A. Černoch, M. Dušek and J. Soubusta, *Experimental implementation of optimal linear-optical controlled-unitary gates*, Physical Review Letters **114**, 153602 (2015), doi:10.1103/PhysRevLett.114.153602.
- [30] A. Babazadeh, M. Erhard, F. Wang, M. Malik, R. Nouroozi, M. Krenn and A. Zeilinger, *High-dimensional single-photon quantum gates: concepts and experiments*, Physical Review Letters **119**, 180510 (2017), doi:10.1103/PhysRevLett.119.180510.
- [31] X. Gao, M. Erhard, A. Zeilinger and M. Krenn, *Computer-inspired concept for high-dimensional multipartite quantum gates*, Physical Review Letters **125**, 050501 (2020), doi:10.1103/PhysRevLett.125.050501.
- [32] Y. Wang, Z. Hu, B. C. Sanders and S. Kais, *Qudits and high-dimensional quantum computing*, Frontiers in Physics **8**, 479 (2020), doi:10.3389/fphy.2020.589504.
- [33] N. J. Cerf, M. Bourennane, A. Karlsson and N. Gisin, *Security of quantum key distribution using d-level systems*, Physical Review Letters **88**, 127902 (2002), doi:10.1103/PhysRevLett.88.127902.
- [34] B. P. Lanyon, T. J. Weinhold, N. K. Langford, J. L. O'Brien, K. J. Resch, A. Gilchrist and A. G. White, *Manipulating biphotonic qutrits*, Physical Review Letters **100**, 060504 (2008), doi:10.1103/PhysRevLett.100.060504.
- [35] M. Malik, M. Erhard, M. Huber, M. Krenn, R. Fickler and A. Zeilinger, *Multiphoton entanglement in high dimensions*, Nature Photonics **10**, 248 (2016), doi:10.1038/nphoton.2016.12.
- [36] Y. Zhang, M. Agnew, T. Roger, F. S. Roux, T. Konrad, D. Faccio, J. Leach and A. Forbes, *Simultaneous entanglement swapping of multiple orbital angular momentum states of light*, Nature Communications **8**, 632 (2017), doi:10.1038/s41467-017-00706-1.
- [37] F. Wang, M. Erhard, A. Babazadeh, M. Malik, M. Krenn and A. Zeilinger, *Generation of the complete four-dimensional Bell basis*, Optica **4**, 1462 (2017), doi:10.1364/OPTICA.4.001462.
- [38] X. M. Hu, Y. Guo, B. H. Liu, Y. F. Huang, C. F. Li and G. C. Guo, *Beating the channel capacity limit for superdense coding with entangled ququarts*, Science Advances **4**, eaat9304 (2018), doi:10.1126/sciadv.aat9304.
- [39] Y. H. Luo, H. S. Zhong, M. Erhard, X. L. Wang, L. C. Peng, M. Krenn, X. Jiang, L. Li, N. L. Liu, C. Y. Lu, A. Zeilinger and J. W. Pan, *Quantum teleportation in high dimensions*, Physical Review Letters **123**, 070505 (2019), doi:10.1103/PhysRevLett.123.070505.

- [40] X. M. Hu, C. Zhang, B. H. Liu, Y. Cai, X. J. Ye, Y. Guo, W. B. Xing, C. X. Huang, Y. F. Huang, C. F. Li and G. C. Guo, *Experimental high-dimensional quantum teleportation*, Physical Review Letters **125**, 230501 (2020), doi:10.1103/PhysRevLett.125.230501.
- [41] V. D’ambrosio, N. Spagnolo, L. Del Re, S. Slussarenko, Y. Li, L. C. Kwek, L. Marrucci, S. P. Walborn, L. Aolita and F. Sciarrino, *Photonic polarization gears for ultra-sensitive angular measurements*, Nature Communications **4**, 2432 (2013), doi:10.1038/ncomms3432.
- [42] Y. Shi, *Both Toffoli and controlled-NOT need little help to do universal quantum computation*, Quantum Information and Computation **3**, 84 (2002), doi:10.1016/S0146-6410(03)00082-6.
- [43] D. G. Cory, M. Price, W. Maas, E. Knill, R. Laflamme, W. H. Zurek, T. F. Havel and S. S. Somaroo, *Experimental quantum error correction*, Physical Review Letters **81**, 2152 (1998), doi:10.1103/PhysRevLett.81.2152.
- [44] M. D. Reed, L. DiCarlo, S. E. Nigg, L. Sun, L. Frunzio, S. M. Girvin and R. J. Schoelkopf, *Realization of three-qubit quantum error correction with superconducting circuits*, Nature **482**, 382 (2012), doi:10.1038/nature10786.
- [45] A. Paetznick and B. W. Reichardt, *Universal fault-tolerant quantum computation with only transversal gates and error correction*, Physical Review Letters **111**, 090505 (2013), doi:10.1103/PhysRevLett.111.090505.
- [46] J. Guillaud and M. Mirrahimi, *Repetition cat qubits for fault-tolerant quantum computation*, Physical Review X **9**, 041053 (2019), doi:10.1103/PhysRevX.9.041053.
- [47] V. V. Shende and I. L. Markov, *On the CNOT-cost of Toffoli gates*, Quantum Information and Computation **9**, 461 (2008), doi:10.1134/S1063779609030058.
- [48] N. Yu, R. Duan and M. Ying, *Five two-qubit gates are necessary for implementing the Toffoli gate*, Physical Review A **88**, 010304(R) (2013), doi:10.1103/PhysRevA.88.010304.
- [49] N. Yu and M. Ying, *Optimal simulation of Deutsch gates and the Fredkin gate*, Physical Review A **91**, 032302 (2015), doi:10.1103/PhysRevA.91.032302.
- [50] E. O. Kiktenko, A. S. Nikolaeva, P. Xu, G. V. Shlyapnikov and A. K. Fedorov, *Scalable quantum computing with qudits on a graph*, Physical Review A **101**, 022304 (2020), doi:10.1103/PhysRevA.101.022304.
- [51] M. Mičuda, M. Sedlák, I. Straka, M. Miková, M. Dušek, M. Ježek and J. Fiurášek, *Efficient experimental estimation of fidelity of linear optical quantum Toffoli gate*, Physical Review Letters **111**, 160407 (2013), doi:10.1103/PhysRevLett.111.160407.
- [52] M. Mičuda, M. Miková, I. Straka, M. Sedlák, M. Dušek, M. Ježek and J. Fiurášek, *Tomographic characterization of a linear optical quantum Toffoli gate*, Physical Review A **92**, 032312 (2015), doi:10.1103/PhysRevA.92.032312.
- [53] S. Ru, Y. Wang, M. An, F. Wang, P. Zhang and F. Li, *Realization of deterministic quantum Toffoli gate with a single photon*, Physical Review A **103**, 022606 (2021), doi:10.1103/PhysRevA.103.022606.

- [54] T. Monz, K. Kim, W. Hänsel, M. Riebe, A. Villar, P. Schindler, M. Chwalla, M. Hennrich and R. Blatt, *Realization of the quantum Toffoli gate with trapped ions*, Physical Review Letters **102**, 040501 (2009), doi:10.1103/PhysRevLett.102.040501.
- [55] I. I. Beterov, I. N. Ashkarin, E. A. Yakshina, D. B. Tretyakov, V. M. Entin, I. I. Ryabtsev, P. Cheinet, P. Pillet and M. Saffman, *Fast three-qubit Toffoli quantum gate based on three-body Förster resonances in Rydberg atoms*, Physical Review A **98**, 042704 (2018), doi:10.1103/PhysRevA.98.042704.
- [56] H. Levine, A. Keesling, G. Semeghini, A. Omran, T. T. Wang, S. Ebadi, H. Bernien, M. Greiner, V. Vuletić, H. Pichler and M. D. Lukin, *Parallel implementation of high-fidelity multiqubit gates with neutral atoms*, Physical Review Letters **123**, 170503 (2019), doi:10.1103/PhysRevLett.123.170503.
- [57] M. J. Gullans and J. R. Petta, *Protocol for a resonantly driven three-qubit Toffoli gate with silicon spin qubits*, Physical Review B **100**, 085419 (2019), doi:10.1103/PhysRevB.100.085419.
- [58] J. Fiurášek, *Linear-optics quantum Toffoli and Fredkin gates*, Physical Review A (6), 062313 (2006), doi:10.1103/PhysRevA.73.062313.
- [59] T. B. Pittman, B. C. Jacobs and J. D. Franson, *Probabilistic quantum logic operations using polarizing beam splitters*, Physical Review A **64**, 062311 (2001), doi:10.1103/PhysRevA.64.062311.
- [60] X. H. Bao, T. Y. Chen, Q. Zhang, J. Yang, H. Zhang, T. Yang and J. W. Pan, *Optical nondestructive controlled-NOT gate without using entangled photons*, Physical Review Letters **98**, 170502 (2007), doi:10.1103/PhysRevLett.98.170502.
- [61] J. P. Li, X. Gu, J. Qin, D. Wu, X. You, H. Wang, C. Schneider, S. Höfling, Y. H. Huo, C. Y. Lu, N. L. Liu, L. Li *et al.*, *Heralded nondestructive quantum entangling gate with single-photon sources*, Physical Review Letters **126**, 140501 (2021), doi:10.1103/PhysRevLett.126.140501.
- [62] W. B. Gao, A. M. Goebel, C. Y. Lu, H. N. Dai, C. Wagenknecht, Q. Zhang, B. Zhao, C. Z. Peng, Z. B. Chen, Y. A. Chen and J. W. Pan, *Teleportation-based realization of an optical quantum two-qubit entangling gate*, Proceedings of the National Academy of Sciences **107**, 20869 (2010), doi:10.1073/pnas.1005720107.
- [63] S. Gasparoni, J. W. Pan, P. Walther, T. Rudolph and A. Zeilinger, *Realization of a photonic CNOT gate sufficient for quantum computation*, Physical Review Letters **93**, 020504 (2004), doi:10.1103/PhysRevLett.93.020504.
- [64] J. Zeuner, A. N. Sharma, M. Tillmann, R. Heilmann, M. Gräfe, A. Moqanaki, A. Szameit and P. Walther, *Integrated-optics heralded controlled-NOT gate for polarization-encoded qubits*, npj Quantum Information **4**, 13 (2018), doi:10.1038/s41534-018-0068-0.
- [65] N. K. Langford, T. J. Weinhold, R. Prevedel, K. J. Resch, A. Gilchrist, J. L. O'Brien, G. J. Pryde and A. G. White, *Demonstration of a simple entangling optical gate and its use in Bell-state analysis*, Physical Review Letters **95**, 210504 (2005), doi:10.1103/PhysRevLett.95.210504.

- [66] N. Kiesel, C. Schmid, U. Weber, R. Ursin and H. Weinfurter, *Linear optics controlled-phase gate made simple*, Physical Review Letters **95**, 210505 (2005), doi:10.1103/PhysRevLett.95.210505.
- [67] R. Okamoto, H. F. Hofmann, S. Takeuchi and K. Sasaki, *Demonstration of an optical quantum controlled-NOT gate without path interference*, Physical Review Letters **95**, 210506 (2005), doi:10.1103/PhysRevLett.95.210506.
- [68] G. F. Viamontes, I. L. Markov and J. P. Hayes, *Quantum circuit simulation*, Springer Science (2009).
- [69] Z. L. Xiang, S. Ashhab, J. Q. You and F. Nori, *Hybrid quantum circuits: Superconducting circuits interacting with other quantum systems*, Reviews of Modern Physics **85**, 623 (2013), doi:10.1103/RevModPhys.85.623.
- [70] G. Waldherr, Y. Wang, S. Zaiser, M. Jamali, T. Schulte-Herbrüggen, H. Abe, T. Ohshima, J. Isoya, J. F. Du, P. Neumann and J. Wrachtrup, *Quantum error correction in a solid-state hybrid spin register*, Nature **506**, 204 (2014), doi:10.1038/nature12919.
- [71] M. J. Peterer, S. J. Bader, X. Jin, F. Yan, A. Kamal, T. J. Gudmundsen, P. J. Leek, T. P. Orlando, W. D. Oliver and S. Gustavsson, *Coherence and decay of higher energy levels of a superconducting transmon qubit*, Physical Review Letters **114**, 010501 (2015), doi:10.1103/PhysRevLett.114.010501.
- [72] T. Bækkegaard, L. B. Kristensen, N. J. S. Loft, C. K. Andersen, D. Petrosyan and N. T. Zinner, *Realization of efficient quantum gates with a superconducting qubit-qutrit circuit*, Scientific Reports **9**, 13389 (2019), doi:10.1038/s41598-019-49657-1.